WRINKLING OF A DEBONDED INITIALLY COMPRESSED $Si_{1-X}Ge_X$ FILM

A. I. Fedorchenko * **A.-B. Wang** *

Institute of Applied Mechanics
National Taiwan University
Taipei, Taiwan 106, R.O.C.

V. I. Mashanov ** **H.-H. Cheng** *

Center for Condensed Matter Sciences
National Taiwan University
Taipei, Taiwan 106, R.O.C.

ABSTRACT

A compressively strained pseudomorphic $Si_{1-x}Ge_x$ film being debonded from Si substrate by selective etching forms wrinkles with a uniform space periodicity. The present study provides experimental evidences and a theoretical model for the wrinkling process. To allow large deflection, non-linear Von Karman plate theory is employed. The amplitude and wavelength of wrinkles are determined by minimizing the total free energy of a debonded wrinkled film. The wrinkling analysis has shown that the amplitude and wavelength of wrinkled film are an outcome of a subtle compromise between bending energy, and normal and shearing components of the stretching energy. The wave number nondimentionalized over the depth of etch is a function of the membrane strain of a bonded film, Poisson's ratio, and the nondimensional film thickness.

Keywords : Thin films; Stress relaxation; Wrinkling; Si-Ge alloys.

1. INTRODUCTION

The film strain is a critical parameter controlling the electrical and optical properties of epitaxial semi-conductor thin films. The $Si_{1-x}Ge_x$ /Si strained layer structures have been used in a wide variety of device such as heterojunction bipolar transistor and heterojunction field effect transistor [1,2]. A wide range of properties can be accessed by manipulating strain in addition to film composition $Si_{1-x}Ge_x$. A novel approach to fabricating semiconductor nanotubes and other shells has been proposed and realized recently [3~5]. This approach is based on the self-rolling of highly strained InGaAs/GaAs and Si-Ge/Si heterostructures detached from a substrate by selective etching, forming a tube-shape scroll. The rate of the lateral etching of the undoped Si buffer layer is thousands times higher than the rate of doping solid solutions Si-Ge so free-standing $Si_{1-x}Ge_x$ films and $Si_{1-x}Ge_x/Si_{1-y}Ge_y$ bifilms can be obtained [4,5]. As a result of etching we obtain two distinct regions: bonded and debonded films which are connected with each other from one side. Our experiments reveal that the debonded film forms wrinkles with a uniform space periodicity, the wrinkles reach an equilibrium configuration, in which the stress is partially relaxed in the film. Experiments show that the wrinkling patterns are common for debonded $Si_{1-x}Ge_x$ film and $Si_{1-x}Ge_x$/ $Si_{1-y}Ge_y$ bifilm. The wavelength of the wrinkling pattern increases from 1.7μm to 6.3μm while the depth of etching increases from 0.8μm to 5.0μm. In each of the cases the deflection exceeds essentially the debonded film thickness. The mechanism of strain relaxation in these debonded films so far is unknown and to the best of our knowledge no work on the debonded film wrinkling in this range of wrinkling pattern parameters has yet been presented in the open literature. At these conditions the debonded film behavior is governed by a set of partial differential equations, known as the Föppl-von Karman equation [6]. These equations are nonlinear, and cannot be solved exactly. Therefore, we use the semianalitical approach similar to the one used recently by Cedra and Mahadevan [7] to quantify the debonded $Si_{1-x}Ge_x$ film wrinkling.

2. EXPERIMENTAL DESCRIPTIONS

$Si_{0.7}Ge_{0.3}$/Si structures were grown by molecular-beam epitaxy on Si (001) substrate on a Riber machine SIVA 32. After a clean surface with a Si (001)-2 × 1 superstructure was obtained, a buffer layer of silicon with thickness of 50nm was grown at a substrate temperature 700°C. This undoped layer of silicon (background concentration was about $4 \times 10^{16}cm^{-3}$) was a sacrificial layer in process of etching. The evaporation of silicon and germanium was carried out from electron-beam evaporators. P-type doping was made by elemental boron from a high temperature cell.

* Professor ** Ph.D.

The buffer layer was coated by highly doped ($p^+ = 5 \times 10^{19}cm^{-3}$) $Si_{0.7}Ge_{0.3}$ layer with thickness of 20nm, which was grown at a temperature of 400°C.

Before etching, films were mechanically scratched such that the etchant could penetrate to the lateral side of the structures. A selective etchant, 3.7 wt.% NH_4OH solution in water, was used at temperatures from 50°C to 75°C [4]. The $Si_{0.7}Ge_{0.3}$ solid solution layers in pseudomorphic, *i.e.*, in compressed state, were possible to be grown at low temperature with small thickness and low content of Ge ($x < 0.4$) [8,9].

Figure 1 shows an atomic force microscopic image of the debonded wrinkled film. It is clearly seen that wrinkles exhibit a good space periodicity. The mechanical properties and parameters of the debonded film shown in Fig. 1 are given in Table 1.

3. WRINKLING ANALYSIS

We consider the case of $Si_{1-x}Ge_x$ film, which were grown by molecular-beam epitaxy on Si (001). Let the film of $Si_{1-x}Ge_x$ before the lateral etching be a flat bi-axially strained plate and take this state of the film as the reference one, in which the membrane strain is ε_0 in both u and v directions. The displacements are set to be zero in this state. After lateral etching of low-doped Si sacrificial layer the debonded part of the film of thickness t, the etching depth h and length L ($t << h << L$) wrinkles assuming a periodic shape. Introducing the coordinate system as shown in Fig. 2, the shape of the wrinkling mode can be described as follows

$$\xi(u, v) = Aw(\eta) \sin(ku), \qquad (1)$$

where ξ is the vertical displacement, $k = 2\pi/\lambda$ is the wave number, λ is the wavelength, A is the constant amplitude of the wrinkles, $\eta = v/h$. The function $w(\eta)$ is normalized to the unity, *i.e.*, $w(1) = 1$.

To allow large deflection, non-linear von Karman plate theory [6] is employed. The nonlinear plate

Table 1 Mechanical properties of debonded $Si_{0.7}Ge_{0.3}$ film

E, 10^{10} N/m^2	ν	A, nm	h, μm	λ, μm	t, nm	ε_0, %
14.9	0.277	70	2.3	3.4	20	1.2

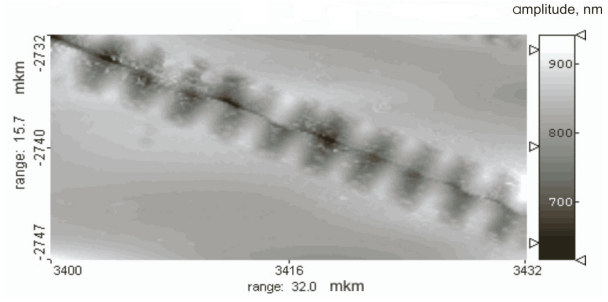

Fig. 1 Atomic force microscopic image of the wrinkling pattern on the debonded part of $Si_{0.7}Ge_{0.3}$ film

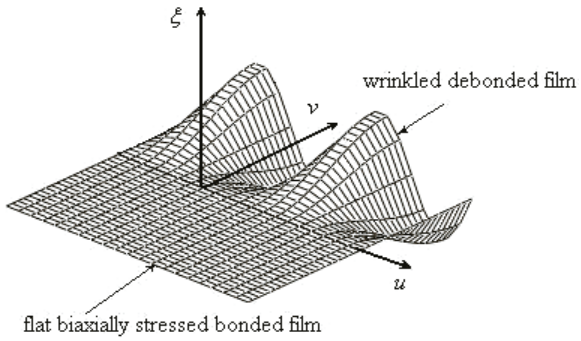

Fig. 2 Sketch of the configuration under consideration along with the used coordinate system

theory includes a term quadratic in the slope of deflection. Neglecting first derivatives of in-plane displacements, the membrane strains in the debonded film can be written as

$$\varepsilon_{ij} = \varepsilon_0 \delta_{ij} + 0.5 \xi_{,i} \xi_{,j}, \qquad (2)$$

where $\varepsilon_0 = (a_{Si} - a_{SiGe})/a_{SiGe}$ is the in-plane coherency strain; a_{Si} (a_{SiGe}) is the lattice parameter of Si ($Si_{1-x}Ge_x$), the tensor suffix $i(j)$ takes the two values u and v. The particular value of the $Si_{1-x}Ge_x$ lattice parameter depends on x and could be determined from Vegard's law: $a_{SiGe} = (1 - x)\, a_{Si} + x a_{Ge}$.

The wavelength and amplitude can be determined by minimizing the total elastic energy F stored in the film. Since in the case under consideration $L >> \lambda$, we can consider the film as infinite in u-direction without loss in generality.

The total energy includes two parts: the pure bending energy, F_b, and the stretching energy, F_s, *i.e.*

$$F = F_b + F_s = \int_0^h \int_0^1 (f_b + f_s)\, du\, dv. \qquad (3)$$

According to Landau and Lifshitz [6] the energy density (energy per unit area) due to bending, f_b, is

$$f_b = 0.5D\,[(\xi_{,uu} + \xi_{,vv})^2 + 2(1-\nu)(\xi_{,uv}{}^2 - \xi_{,uu}\,\xi_{,vv})], \qquad (4)$$

where $D = Et^3/[12(1-\nu^2)]$ is the flexural rigidity of the elastic film.

The energy density due to stretching, f_s is

$$f_s = 0.5\, M_{ij}\, \varepsilon_{ij}. \qquad (5)$$

Hooke's law relates the membrane forces M_{ij} in the film to the membrane strains, namely

$$M_{ij} = Et\,[\varepsilon_{ij}/(1+\nu) + \nu\, \varepsilon_{kk}\delta_{ij}/(1-\nu^2)], \qquad (6)$$

where E is Young's modulus, ν is Poisson's ratio.

In the reference state $M_{uu} = M_{vv} = \sigma_0 t$ and $M_{uv} = 0$, where $\sigma_0 = E\varepsilon_0/(1-\nu)$ is the biaxial stress. Consequently, the stretching energy in this state is $f_{s0} = Et\,\varepsilon_0^2/(1-\nu)$.

The relaxation of debonded film in the u- and

v-directions is accompanied by wrinkling and, consequently, acquiring some bending energy and energy caused by appearance of the shearing stress and strain. Thus, the amplitude and wavelength of a wrinkled film are an outcome of the trade-off between bending energy, and normal and shearing components of the stretching energy. Two distinct regions can be identified: bonded and debonded films. On the boundary of these two zones ($\eta = 0$) the clamped boundary conditions are

$$w(0) = w'(0) = 0 . \tag{7}$$

On the free edge of the debonded film ($\eta = 1$) the boundary conditions are [6]

$$w''(1) - \nu k^{*2} w(1) = 0, \quad w'''(1) - (2-\nu) k^{*2} w'(1) = 0 , \tag{8}$$

where $k^* = kh$ is the dimensionless wave number.

Before deriving the total energy of the film, let us notice that the debonded film wrinkles laterally (in u-direction) to reduce the elastic energy due to compressive stress $\sigma_0 \sim \varepsilon_0/(1-\nu)$ in the vicinity of the clamped boundary. Therefore, it is reasonable to assume that the following relation determines the amplitude and wavelength of the wrinkle

$$-\varepsilon_0 / (1-\nu) \approx A^{*2}(k^{*2} + \nu) , \tag{9}$$

where $A^* = A/h$ is the dimensionless amplitude of the wrinkle.

Equation (8) correlates well with experimental data given in Table 1.

Plugging Eq. (2) into Eq. (3) and accounting for Eqs. (1), (3)-(6) yields

$$F \sim \frac{Eth}{(1-\nu^2)} \left[\frac{(2+\nu)}{2} \varepsilon_0 A^{*2} + \frac{(2-\nu)}{2} (A^{*2} k^*)^2 + A^{*4} + \frac{t^{*2}}{12} (A^* k^{*2})^2 \right], \tag{10}$$

where $t^* = t/h$.

In deriving Eq. (10) we have omitted the constant term and terms proportional to second and fourth power of $A^* k^*$, since they close to constants as it follows from Eq. (9) and, consequently, do not influence on the minimum value of F. To evaluate the integrals over η from 0 to 1, we used the polynomial fit to $w(\eta)$, the coefficients of which were founded by means of the boundary conditions given by Eqs. (7) and (8).

By virtue of Eq. (9), Eq. (10) can be rewritten as

$$F \sim \underbrace{\frac{(2+\nu)}{2} \frac{\varepsilon_0}{k^{*2}+\nu}}_{F1} \underbrace{- \frac{(2-\nu)}{2(1-\nu)} \frac{k^{*2} \varepsilon_0}{(k^{*2}+\nu)^2}}_{F2} \underbrace{- \frac{\varepsilon_0}{(1-\nu)(k^{*2}+\nu)^2}}_{F3} + \underbrace{\frac{t^{*2}}{12} \frac{k^{*4}}{k^{*2}+\nu}}_{F4} . \tag{11}$$

Figure 3 demonstrates the variation of the terms $F1$-$F4$ in Eq. (11) with the dimensionless wave number k^*. The $F1$ and $F3$ represent the normal components of the stretching energy, $F2$ stands for the shearing one, and $F4$ represents the bending energy. As seen from Fig. 3, upon the film relaxation the shearing component of the stretching energy $F2$ increases and takes a maximum value at $k^* \approx 0.5$. An important point is that the bending energy alone cannot be neglected in spite of the fact that its value is relatively small due to the smallness of the dimensionless film thickness squared, $t^{*2} = 7.6 \times 10^{-5}$. In this case the function $F1 + F2 + F3$ does not have a minimum value and approaches zero asymptotically. Neglecting both $F2$ and $F4$ yields a minimum at $k^* = 1.5$, but this value differs essentially from the experimental one.

The foregoing shows plainly that all terms in Eq. (11) play an important role and have to be taken into account. Minimizing Eq. (11) with respect to k^* gives $k^* = 4.2$ and, correspondingly, Eq. (9) gives $A^* = 0.03$. For dimension wavelength and amplitude we have $\lambda = 3.4\mu m$ and $A = 0.07\mu m$, respectively. The results agree well with the experimental data from Table 1.

Figure 4 shows the effect of the depth of etching on equilibrium values of the wavelength and amplitude of wrinkles. The measured wavelength and amplitude for $h = 2.3$ from Table 1 are also added for comparison. At $h = 1\mu m$ the values of the wavelength and amplitude are $2.02\mu m$ and $41nm$, respectively, whereas at $h = 6\mu m$ the ones are $6.13\mu m$ and $127nm$, respectively. Both the wavelength and amplitude increase with depth of etching, the former as $2.03h^{0.62}$ and the latter as $41.71h^{0.62}$.

As Eq. (11) suggests, the initial epitaxial strain ε_0 could have an important effect on the amplitude and wavelength of the wrinkles. To clear up this issue, we have found the minima of Eq. (11) for different ε_0-values at the same Poisson's ratio. It should be noted here that practically we can vary ε_0 only by the change the epitaxial layer $Si_{1-x}Ge_x$ lattice parameter a_{SiGe}, *i.e.*, by means of the change in the parameter p value. But the wide-ranging change the x may result in the change the ν. Taking $\nu = 0.278$ for Si and 0.273 for Ge [10], Poisson's ratio x-dependence could be described by the following linear interpolation formula:

$$\nu = 0.278 - 0.005x . \tag{12}$$

Table 2 displays the effect of the ε_0 on the wavelength and amplitude of the wrinkles. While x varies in a wide range from 0.1 to 0.5, Poisson's ratio changes weakly from 0.278 to 0.276 according to Eq. (12). Therefore, all calculations were carried out at the same $\nu = 0.277$, which corresponds to $x = 0.3$. As evident from Table 2, the initial epitaxial strain affects the amplitude of wrinkles strongly, whereas the wavelength varies relatively slightly. Fivefold increasing the ε_0 modulus from 0.4% to 2.1% causes an increase in the amplitude of wrinkles by 66%, at the same time the wavelength decreases by 26%.

Table 2 Effect of the initial epitaxial strain ε_0 on the wavelength and amplitude of the wrinkles. The ν- and t^*-values correspond to those from Table 1.

x	ε_0, %	k^*	λ, μm	A, nm
0.1	– 0.4	3.5	4.2	50
0.2	– 0.8	3.9	3.7	62
0.3	– 1.2	4.2	3.4	70
0.4	– 1.7	4.5	3.2	77
0.5	– 2.1	4.8	3.1	83

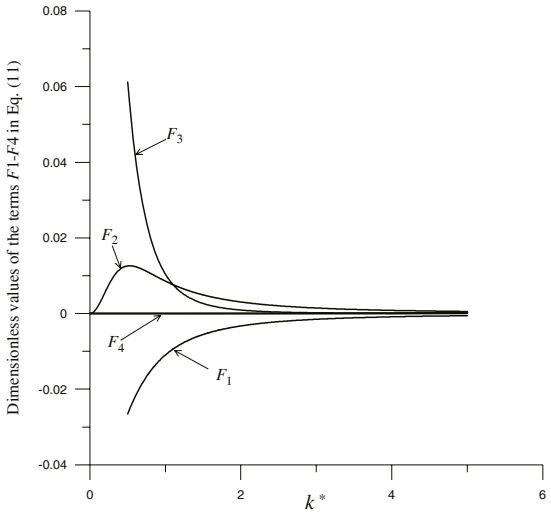

Fig. 3 Variation of terms $F1$-$F4$ in Eq. (11) with the dimensionless wave number k^*

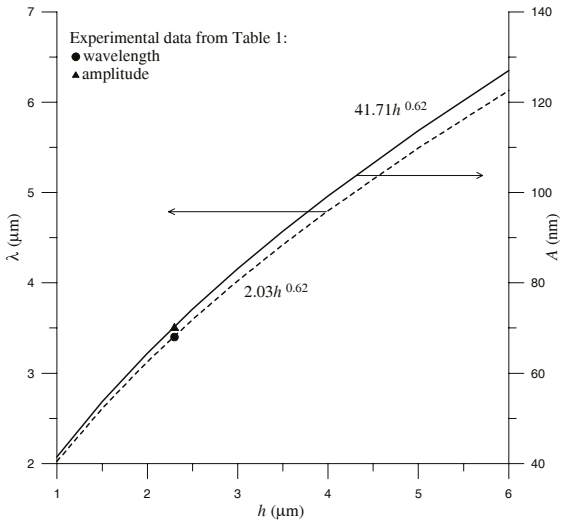

Fig. 4 Variation of an equilibrium wavelength λ (dash line) and amplitude A (solid line) of the wrinkles with the depth of etching h

4. CONCLUSIONS

In the present study experimental observations are provided for the debonded $Si_{1-x}Ge_x$ film wrinkling. The film was grown by molecular-beam epitaxy on Si (001). Bonded to substrate the film presents a flat bi-axially compressed plate. After the lateral etching the debonded part of the film forms the wrinkle pattern with a uniform space periodicity. The quantitative analysis of the debonded film relaxation, which results in wrinkling, is carried out. The wrinkling analysis has shown that the amplitude and wavelength of wrinkled film are an outcome of a subtle trade-off between bending energy, and normal and shearing components of the stretching energy. The wave number nondimentionalized over the depth of etching is a function of the membrane strain of a bonded film, Poisson's ratio, and the nondimensional film thickness. Both the wavelength and amplitude of wrinkles increase with the depth of etching as $h^{0.62}$. Theoretical analysis has revealed that the initial epitaxial compressive strain ε_0 effects on both the amplitude of wrinkles and their wavelength. The amplitude increases with increasing ε_0 and at the same time the wavelength decreases.

Theoretical predictions of the wavelength and amplitude of wrinkles agree well with experimental data from this study.

ACKNOWLEDGENTS

The authors would like to thank the National Science Council of the Republic of China for financial support this research under Grant No. NSC92-2811-M-002- 029.

REFERENCES

1. Jain, S. C., Decoutere, S. Willander, M. and Maes, H. E., "SiGe HBTs for Applications in BiCMOS Technology: I. Stability, Reliability and Material Parameters," *Semicond. Sci. and Technol.*, 16, pp. R51–R65 (2001).
2. Schaffler, F., "High-Mobility Si and Ge Structures," *Semicond. Sci. and Technol.*, 12, pp. 1515–1549 (1997).
3. Prinz, V. Y., Seleznev, V. A., Gutakovsky, A. K., Chehovskiy, A. V., Preobrazhenskii, V. V., Putyato, M. A. and Gavrilova, T. A., "Free-Standing and Overgrown InGaAs/GaAs Nanotubes, Nanohelices and Their Arrays," *Physica E*, 6, pp. 828–831 (2000).
4. Golod, S. V., Prinz, V. Ya., Mashanov, V. I. and Gutakovsky, A. K., "Fabrication of Conducting GeSi/Si Micro- and Nanotubes and Helical Microcoils," *Semicond. Sci. and Technol.*, 16, pp.181–185 (2001).
5. Prinz, V. Ya., Golod, S. V., Mashanov, V. I. and Gutakovsky, A. K., "Free-Standing Conductive GeSi/Si Helical Microcoils, Micro- and Nanotubes," *Proc. 26th Int. Symp. Compound Semiconductors*, Berlin, Germany, Inst. Phys. Conf. Ser., 166, pp. 203–206 (2000).

6. Landau, L. D. and Lifshitz, E. M., *Theory of Elasticity*, Pergamon, New York (1986).
7. Cerda, E. and Mahadevan, L., "Geometry and Physics of Wrinkling," *Phys. Rev. Lett*., 90, 074302 (2003).
8. People, R. and Bean, J. C., "Calculation of Critical Layer Thickness versus Lattice Mismatch for Ge_xSi_{1-x}/Si Strained-Layer Heterostructures," *Appl. Phys. Lett*., 47, pp. 322–324 (1985).
9. Bai, G., "Strain Relief of Metastable GeSi Layers on Si(100)," *J. Appl. Phys*., 75, pp. 4475–4481 (1994).
10. Brunner, K., "Si/Ge Nanostructures," *Rep. Prog. Phys*., 65, pp. 27–79 (2002).

(Manuscript received August 13, 2004,
accepted for publication January 11, 2005.)